

# A comparative high-resolution spectroscopic study of the Hyades giants $\gamma$ Tauri and $\epsilon$ Tauri

G. Smith

Department of Physics, Nuclear and Astrophysics Laboratory, Keble Road, Oxford, OX1 3RH, UK

Received 21 April 1999 / Accepted 30 August 1999

**Abstract.** Spectra of the Hyades K0 giants  $\gamma$  Tau and  $\epsilon$  Tau in the regions 5852–5864 Å and 6145–6176 Å have been recorded at high resolution and with signal/noise in the range 150–250. A critical comparison reveals that, although nearly all lines in the observed regions have a similar depth, lines of  $\epsilon$  Tau are broader by about 10% than those of  $\gamma$  Tau. An LTE analysis indicates that slightly higher turbulent broadening in  $\epsilon$  Tau can account for the observed differences in line-width. Study of two particularly temperature sensitive features confirms earlier observations that the effective temperature of  $\epsilon$  Tau is less than that of  $\gamma$  Tau and determines the temperature difference to be  $80 \pm 20$  K.

**Key words:** stars: abundances – stars: fundamental parameters – stars: individual:  $\gamma$  Tau – stars: individual:  $\epsilon$  Tau – stars: late-type

## 1. Introduction

As part of a long-running programme of high-resolution spectroscopy of bright late-type stars, spectral regions around 6000 Å in the spectra of the Hyades K0 giants  $\gamma$  Tau and  $\epsilon$  Tau have been observed with a resolution limit of 0.05 Å (full-width at half-maximum). At this resolution line profiles are reasonably well resolved and, although the two spectra are very similar, it is possible to distinguish differences in both surface temperature and turbulent broadening between the two stars. In the present paper we illustrate these differences and discuss their interpretation.

## 2. Observations and data reduction

Observations of  $\gamma$  Tau and  $\epsilon$  Tau were made at the McDonald Observatory on 1–4 November, 1991, by G. Smith and M.J. Ruck (University of Oxford) and J. Tomkin (University of Texas), using the 2.7 m telescope and coudé spectrograph equipped with an 800 × 800 pixel CCD detector. We observed spectral regions covering approximately 12 Å each centred on 5858, 6151, 6162, 6170 Å. These observations made use of an échelle grating giving a dispersion of about 0.014 Å per diode (15 μm). The required order of the échelle spectrum was isolated before entering

the main spectrograph by means of a grating monochromator. This arrangement, in which only about 100 Å of spectrum enters the main spectrograph, is particularly effective in reducing the scattered-light background. As a test for scattered light, recordings were made of the skylight spectrum in the same spectral regions. Subsequent measurements of equivalent widths for representative spectral lines showed that these equivalent widths differed by less than 2% from those measured from the high dispersion spectral atlas of Kurucz et al. (1984). These differences are within the errors of measurement and certainly less than the likely errors arising from blending in the spectra of the Hyades giants. Scattered light was therefore assumed to be negligible. The entrance slit-width of 240 μm projected on to 3.6 diodes in the focal plane which at 6000 Å gave a resolution limit of  $\simeq 0.05$  Å. A recording of a Th-Ar lamp spectrum showed that the instrumental profile could be well represented by a Gaussian function with a full-width at half-maximum intensity equal to the projected slit width. Integration times of 15–20 min yielded spectra with signal/noise in the range 150–250 in “seeing” of typically 2–3 arcsec. The spectrum of a tungsten filament lamp, used for subsequent flat-field correction, was recorded at the same grating setting immediately after each stellar integration. Initial data reduction was undertaken at the Department of Astronomy, University of Texas at Austin. Further analysis and measurement were carried out at Oxford using the standard Starlink package DIPSO.

## 3. Analysis

The analysis has been carried out by comparing the observed spectra with synthetic spectra calculated in the LTE approximation using model atmospheres. The spectral regions chosen for observation contain numerous lines of iron and calcium for which accurate atomic data are available. Atomic data for Ca I lines was taken from the laboratory work of Smith & Raggett (1981). Atomic data for other lines was determined by fitting synthetic spectra, calculated using the Holweger-Müller solar atmosphere (Holweger & Müller 1974), to the corresponding regions of the solar spectrum. Our ‘solar’ oscillator strength for the Fe II line at 6149.25 Å agrees very closely with the value,  $-2.837$ , recently obtained by Raassen & Uylings (1998) using a sophisticated theoretical method. The question of the most

*Send offprint requests to:* G. Smith

appropriate type of model atmosphere for late-type giant stars was considered by Drake & Smith (1991) in a critical analysis of features in the spectrum of the K0 giant, Pollux ( $\beta$  Gem). Using the profile of the Ca II 8542 Å line as a feature to test the temperature structure of the atmosphere, these authors concluded that a model from the MARCS suite of atmospheres (Bell et al. 1976) produced a theoretical line shape in best agreement with the observed profile. These atmospheres have been used successfully in a recent study of the G8 giants,  $\mu$  Peg and  $\lambda$  Peg (Smith 1998) and, even more pertinently, to derive the overall metallicity and surface gravity for the two Hyades stars under study here, using only the wings of the strong lines of Ca II at 8542 Å and Mg I at 8806 Å (Smith & Ruck 1997). This last paper adopted effective temperatures from the infrared flux method (Blackwell & Lynas-Gray 1998) and obtained the following optimum set of atmospheric parameters:

|  | $\gamma$ Tau     | $\epsilon$ Tau   |
|--|------------------|------------------|
| $T_{\text{eff}}$ (K)                   | $4965 \pm 40$    | $4911 \pm 35$    |
| $\log g$ ( $g$ in $\text{cm s}^{-2}$ ) | $2.65 \pm 0.20$  | $2.45 \pm 0.20$  |
| [M/H]                                  | $+0.12 \pm 0.03$ | $+0.15 \pm 0.03$ |

MARCS atmospheres corresponding to the above sets of parameters were adopted in the present study. Our values for metallicity are very close to the value, [M/H] = +0.14, chosen as representative of modern analyses of Hyades cluster stars in the recent exhaustive study resulting from observations made by the Hipparcos satellite (Perryman et al. 1998). Our stellar spectra are broadened by turbulence which must be included in the synthesis for a realistic comparison between computed and observed profiles. Turbulence on small scales (microturbulence) broadens the atomic absorption coefficient and may be determined using equivalent widths of relatively unblended lines (see next section). Turbulence on large scales (macroturbulence) may, in the present case, be sufficiently well accounted for by applying a Gaussian smoothing function to the synthesised spectra. In reality this smoothing function also includes instrumental and rotational broadening but instrumental broadening (equivalent to a Gaussian broadening parameter of  $1.5 \text{ km s}^{-1}$  at 6000 Å) has a small effect compared to macroturbulence ( $3.0$  to  $4.0 \text{ km s}^{-1}$ ) and rotational broadening is expected to be small in giant stars of spectral type K0. Macroturbulence and rotation are discussed further in Sect. 5.

#### 4. Results

As would be expected for two stars with such closely similar parameters, the observed spectra in all the regions investigated are very similar. A critical comparison reveals, however, that, although the depths of nearly all lines are almost identical, line profiles in  $\epsilon$  Tau are broader by about 10% than those in  $\gamma$  Tau. This is illustrated in Fig. 1, which shows the region between 6148.5 and 6152.5 Å, and Fig. 2, which shows the region between 6160.5 and 6164.5 Å. In both figures the observed spectra are superimposed and plotted with their continua set to 1.0. In all of the regions investigated only two major features show

**Table 1.** Atomic data and equivalent widths for lines of Fe I, Fe II and Ca I in the spectra of  $\gamma$  Tau and  $\epsilon$  Tau

| Wavelength (Å) | Excitation (eV) | $\log gf^{\text{a}}$ | Equivalent width (mÅ) |                |
|----------------|-----------------|----------------------|-----------------------|----------------|
| Fe I           |                 |                      | $\gamma$ Tau          | $\epsilon$ Tau |
| 5855.09        | 4.61            | -1.52                | 49                    | 54             |
| 5856.10        | 4.29            | -1.55                | 66                    | 74             |
| 5858.79        | 4.22            | -2.20                | 40                    | 45             |
| 5859.60        | 4.55            | -0.60                | 105                   | 110            |
| 5862.37        | 4.55            | -0.39                | 117                   | 123            |
| 6151.62        | 2.18            | -3.30*               | 101                   | 113            |
| 6157.73        | 4.07            | -1.21                | 96                    | 105            |
| 6159.38        | 4.61            | -1.85                | 38                    | 43             |
| 6165.36        | 4.14            | -1.47                | 78                    | 87             |
| 6173.34        | 2.22            | -2.88*               | 119                   | 133            |
| Fe II          |                 |                      |                       |                |
| 6149.25        | 3.89            | -2.85                | 53                    | 56             |
| Ca I           |                 |                      |                       |                |
| 6156.03        | 2.52            | -2.45                | 33                    | 38             |
| 6161.29        | 2.52            | -1.27                | 101                   | 112            |
| 6163.75        | 2.52            | -1.29                | 100                   |                |
| 6166.44        | 2.52            | -1.14                | 108                   | 117            |
| 6169.04        | 2.52            | -0.80                | 128                   | 140            |
| 6169.56        | 2.53            | -0.48                | 147                   | 159            |

<sup>a</sup> Values for Fe lines are derived from the solar spectrum (see text) apart from those marked (\*) which are laboratory measurements from Blackwell et al. (1982); values for Ca lines are laboratory measurements from Smith & Raggett (1981).

significant differences between  $\gamma$  Tau and  $\epsilon$  Tau. These features are the V I line at 6150.15 Å (see Fig. 1) and the blend of Ni I, Fe I and Ca I lines at about 6163.5 Å (see Fig. 2). The strengths of the V I and Ni I lines are particularly temperature sensitive and the observed differences between the two stars result from the slightly lower surface temperature of  $\epsilon$  Tau, as indicated by application of the infrared flux method (see previous section). An increase in turbulent broadening can account for the broader profiles in  $\epsilon$  Tau as will be explained below.

In order to make a more quantitative comparison of the two spectra, we have calculated synthetic spectra for  $\gamma$  Tau and  $\epsilon$  Tau using MARCS atmospheres and the parameters listed in the previous section. Our synthetic spectra included all known metal lines and CN molecular lines taken from the very extensive computations of Jørgensen & Larsson (1990) which were kindly made available to us by the authors. We have no independent information on CNO abundances but the CNO abundances determined by Gratton & Ortolani (1986) were found to predict molecular features closely similar to those observed.

The microturbulence parameter,  $\xi$ , may be determined, independently of macroturbulence, from equivalent widths of relatively unblended lines. Equivalent widths for Fe I, Fe II and Ca I lines are shown in Table 1. Weak blends have been removed from the line wings following the method described by Smith et al. (1992). The broader profiles of lines in  $\epsilon$  Tau show up as larger equivalent widths relative to  $\gamma$  Tau. There are no measure-

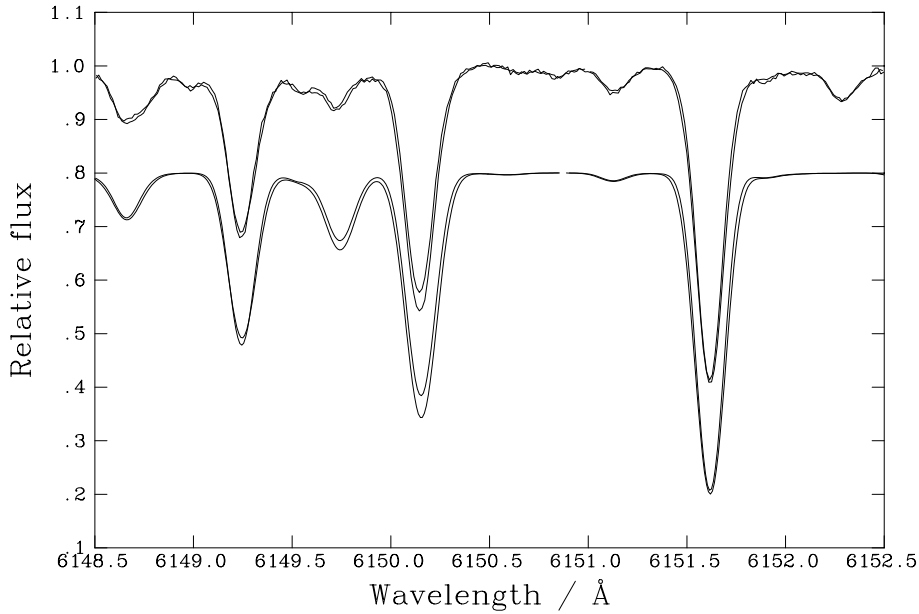


**Fig. 1.** Comparison between spectra of  $\gamma$  Tau and  $\epsilon$  Tau in the region of 6150 Å: observed spectra with continua set to 1.0; synthetic spectra with continua displaced lower by 0.2. In both cases the line profiles corresponding to  $\epsilon$  Tau are slightly broader.

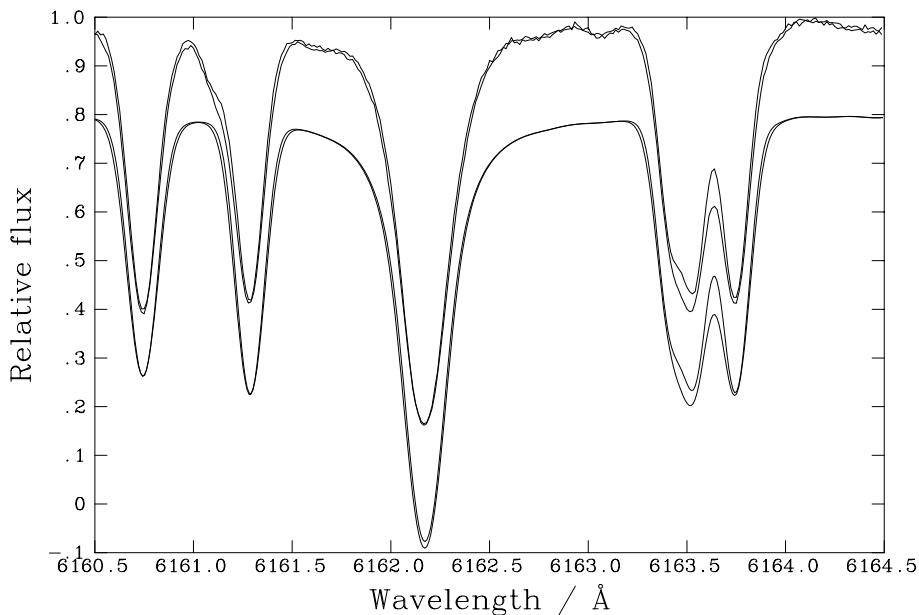


**Fig. 2.** Comparison between spectra of  $\gamma$  Tau and  $\epsilon$  Tau in the region of 6162 Å: observed spectra with continua set to 1.0; synthetic spectra with continua displaced lower by 0.2. In both cases the line profiles corresponding to  $\epsilon$  Tau are slightly broader.

ments of similar accuracy to compare with our results but the tendency for lines of  $\epsilon$  Tau to have larger equivalent widths than those of  $\gamma$  Tau is present in the earlier work, based on photographic spectra, of Helfer & Wallerstein (1964). These authors, together with Griffin (1969) who only studied  $\gamma$  Tau, also obtained equivalent widths of similar magnitude for the very few lines which overlap our data set. Gray & Endal (1982), in a study of macroturbulence and rotation in the Hyades giants, list equivalent widths for a group of metallic lines in the region of 6250 Å. Their spectra were of similar quality to our own (limit of resolution  $\sim 2.5 \text{ km s}^{-1}$ ) and their equivalent widths mostly show similar differences between  $\gamma$  Tau and  $\epsilon$  Tau. However, these equivalent widths were not used for an abundance analysis and Gray (1982a), in another paper using the same analytical

techniques, cautions that his equivalent widths are intended only as a guide to illustrate differing line strengths.

Using model atmospheres corresponding to our optimum parameters, we constructed loci of constant equivalent width on a graph of  $[\text{Fe}/\text{H}]$ , logarithmic abundance of iron relative to the Sun, against microturbulence,  $\xi$ , for each star. These graphs are shown in Fig. 3. The loci should intersect in a narrow region defining appropriate values of  $[\text{Fe}/\text{H}]$  and  $\xi$ . Most of the lines featured in Fig. 3, those with steep gradients, are extremely sensitive to turbulent broadening. The weakest lines, which define the region of intersection most clearly, are those with the largest uncertainties in their equivalent widths. In order to determine the optimum values of  $[\text{Fe}/\text{H}]$  and  $\xi$ , we have calculated the mean abundance and standard deviation of the mean as a function of microturbulence. The optimum values are

taken to be those corresponding to the minimum standard deviation which yields the following reasonably well defined results:

$$\begin{aligned} \gamma \text{ Tau } [\text{Fe}/\text{H}] &= +0.150 \pm 0.029; \quad \xi = 1.32 \text{ km s}^{-1} \\ \epsilon \text{ Tau } [\text{Fe}/\text{H}] &= +0.163 \pm 0.030; \quad \xi = 1.47 \text{ km s}^{-1} \end{aligned}$$

The iron abundances, relative to the Sun, are very close to the overall metallicities found by Smith & Ruck (1997), who used strong-line wing profiles. The broader profiles found in  $\epsilon$  Tau appear to result from a slightly larger turbulent broadening. Gray & Endal (1982) found microturbulence values in the range  $\sim 1.5\text{--}1.8 \text{ km s}^{-1}$  for the Hyades giants (no values quoted for individual stars). Their somewhat hazardous method, based on locating the first zero in the Fourier amplitude of the line profile, could only be applied to the strongest lines in their sample and is unlikely to be as precise as the direct method adopted here. The microturbulence values we have determined are very close to the value,  $1.4 \pm 0.1 \text{ km s}^{-1}$ , derived using similar techniques for the stars  $\mu$  Peg (Smith 1998) and  $\beta$  Gem (Drake & Smith 1991), which are at a similar stage of evolution.

Having determined the microturbulence and metallicity, we were able to determine the additional broadening by applying a Gaussian smoothing function to the synthesised spectra so as to bring observed and computed line profiles into agreement. This procedure yielded, for  $\gamma$  Tau, a Gaussian broadening parameter of  $3.6 \pm 0.1 \text{ km s}^{-1}$  and, for  $\epsilon$  Tau, a Gaussian broadening parameter of  $4.0 \pm 0.1 \text{ km s}^{-1}$ . Recalling that part of this broadening was due to an instrumental component equivalent to a Gaussian broadening parameter of  $1.5 \text{ km s}^{-1}$ , the true additional broadening, arising from macroturbulence and rotation, becomes, for  $\gamma$  Tau,  $3.3 \pm 0.1 \text{ km s}^{-1}$  and, for  $\epsilon$  Tau,  $3.7 \pm 0.1 \text{ km s}^{-1}$ . These values are directly comparable with the values,  $3.0 \pm 0.1 \text{ km s}^{-1}$  and  $7.6 \pm 0.5 \text{ km s}^{-1}$ , found by Smith (1998) for the G8 III star,  $\mu$  Peg, and the G8 II star,  $\lambda$  Peg, respectively; also with the value,  $3.5 \pm 0.5 \text{ km s}^{-1}$ , found by Drake & Smith (1991) for the K0 III star,  $\beta$  Gem.

The two best-fit synthetic spectra for the 6151 Å and 6162 Å regions are shown superimposed with their continua displaced downwards by 0.2 relative to the observed spectra in Figs. 1 and 2. It can be seen that the synthetic spectra reflect accurately the differences between the observed spectra both as regards the differences in line profiles and as regards the temperature dependent features. Fig. 4 shows a comparison between observed and calculated spectra for both stars in the region 6148.5–6152.5 Å. The figure illustrates the quality of fit to major spectral features that was obtained for all the regions studied.

The temperature dependent features indicate a temperature difference between the two stars of  $80 \pm 20 \text{ K}$ , slightly larger than the difference in effective temperature,  $54 \pm 50 \text{ K}$ , resulting from the application of the infrared flux method but well within the error limits. Gray (1992, chapter 15) has already pointed out that line-depth ratios for species such as V I and Fe I can yield resolution on the temperature coordinate of 10–15 K. In Gray (1989) a V I/Fe I line-depth ratio is used to order a large

sample of G giants into a monotonic temperature sequence with much better temperature resolution than can be achieved using colour indices. The higher effective temperature of  $\gamma$  Tau relative to  $\epsilon$  Tau is apparent from Table 2 of this paper though the quoted line-depth ratios are not translated into a quantitative temperature difference. It should be borne in mind that the temperature-dependent features are formed at higher levels in the photosphere than the continuum which determines the effective temperature. We also note that the relative strengths of the Fe I 6151.62 Å line and the Fe II 6149.25 Å line in both stars are well reproduced by our computed spectra, providing further justification for our choice of effective temperatures.

Apart from the weak 6156.03 Å line which is unreliable because of blending, all of our Ca I lines are similarly sensitive to turbulence and do not define unique values of [Ca/H] and  $\xi$  in an abundance-microturbulence plot. If we assume the values of  $\xi$  found for iron lines, the indicated values of [Ca/H] are  $+0.15 \pm 0.03$ , for  $\gamma$  Tau, and  $+0.18 \pm 0.04$ , for  $\epsilon$  Tau, in good agreement with the relative abundances found by other methods.

## 5. Discussion

The use of a Gaussian smoothing function to represent the combined effects of macroturbulence and rotation, while convenient and giving a good representation of the observed profiles apart from the line wings all of which are blended to some extent, may be criticised on physical grounds. Turbulent motions in the solar photosphere are clearly anisotropic and many investigations of macroturbulent broadening have adopted the radial-tangential model of Gray (1975). This model assumes turbulent motions with a Gaussian dispersion in only the radial and tangential directions and, in order to obtain quantitative results, it is usual to assume equal dispersions and equal areas of the stellar surface associated with each motion. Gray (1992, chapter 18) describes this approach and provides a method for separating rotational and turbulent broadening using Fourier techniques. Gray & Endal (1982), using this method, determined the rotational broadening parameter for both  $\gamma$  Tau and  $\epsilon$  Tau to be  $v \sin i = 3.4 \text{ km s}^{-1}$  and the radial-tangential macroturbulence dispersions,  $\zeta_{\text{RT}}$ , to be 4.6 and  $4.8 \text{ km s}^{-1}$  respectively. These figures were subsequently revised by Gray (1982b) to  $v \sin i = 2.4 \text{ km s}^{-1}$ ,  $\zeta_{\text{RT}} = 5.9 \text{ km s}^{-1}$ , for  $\gamma$  Tau, and  $v \sin i = 2.5 \text{ km s}^{-1}$ ,  $\zeta_{\text{RT}} = 6.2 \text{ km s}^{-1}$ , for  $\epsilon$  Tau, following the discovery that weak lines (equivalent width  $W_\lambda < 100 \text{ mÅ}$ ) and strong lines ( $W_\lambda > 100 \text{ mÅ}$ ) indicated different values of macroturbulence.

Most of the line profiles in our sample are too perturbed by blends in the line wings to justify application of the more elaborate analysis using Fourier techniques. Gray (1992, chapter 18, p 411) states that when rotational and macroturbulent broadening are similar in magnitude, the combined effects produce a profile that is close to Gaussian, which is the justification for the approach adopted in the present paper. However, in order to relate our results more closely to those of Gray (1982b), we have applied the Fourier technique to the profile of the Fe I

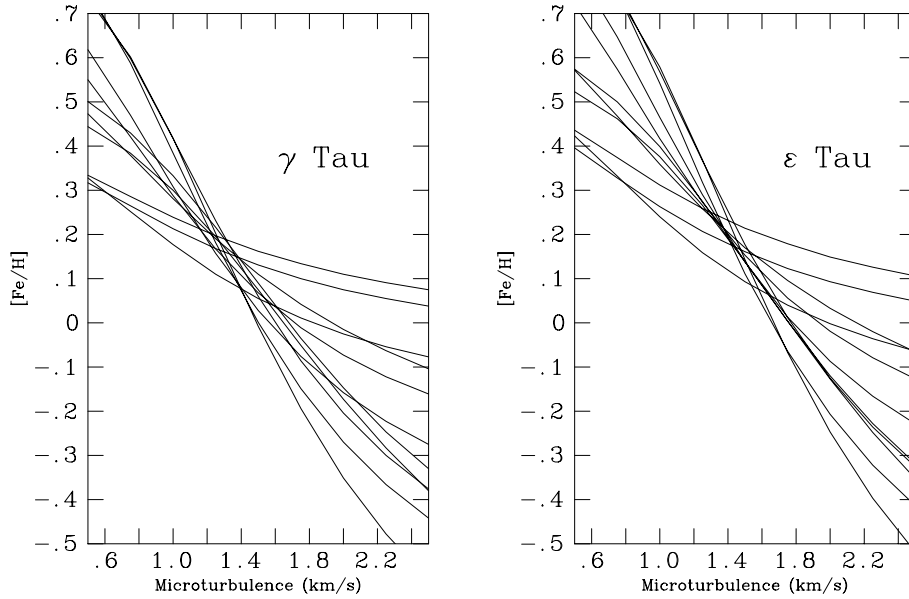


**Fig. 3.** Logarithmic abundance of iron, relative to the Sun, as a function of microturbulence for the iron lines listed in Table 1.

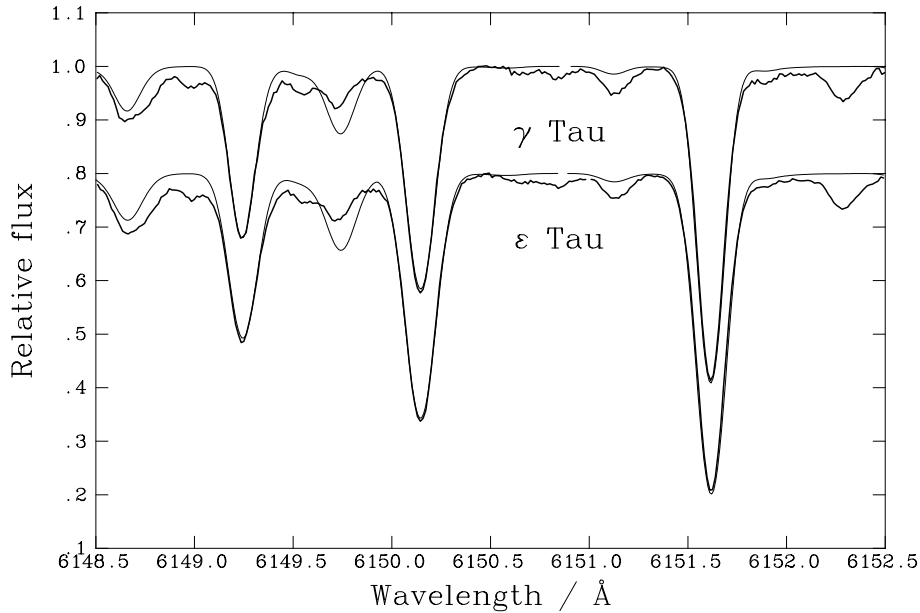


**Fig. 4.** Comparison between observed (bold line) and synthetic spectra for  $\gamma$  Tau and  $\epsilon$  Tau (ordinates displaced lower by 0.2) in the region of 6150 Å.

6151.62 Å line (see Fig. 4): this profile is judged to be the one least affected by blends. For both  $\gamma$  Tau and  $\epsilon$  Tau, we obtain  $v \sin i = 1$  to  $2 \text{ km s}^{-1}$  and  $\zeta_{\text{RT}} \approx 6 \text{ km s}^{-1}$ , with uncertainty  $\approx 0.5 \text{ km s}^{-1}$ . The radial-tangential macroturbulence is close to that obtained by Gray though the rotational broadening appears to be somewhat lower. Gray was able to achieve impressive consistency by averaging Fourier amplitudes for a sample of 11 lines carefully selected for minimum blending. The spectral lines studied in the present paper have been used in several previous abundance analyses and were originally chosen on grounds of good quality atomic data. Rotational and macroturbulent broadening cannot be unambiguously separated using the present data. A test calculation for Fe I 6151.62 Å shows that a profile calculated with  $v \sin i = 2.5 \text{ km s}^{-1}$  and a Gaussian macroturbulence dispersion of  $2.9 \text{ km s}^{-1}$  is indistinguishable

from a profile calculated with an overall Gaussian broadening parameter of  $3.3 \text{ km s}^{-1}$ , the best fit value for  $\gamma$  Tau. However, the results of Gray (1982b) and the above-mentioned analysis of the 6151.62 Å line profile suggest that macroturbulence is likely to be the dominant broadening factor. This being the case, it seems likely that the slightly greater microturbulence found for  $\epsilon$  Tau, relative to  $\gamma$  Tau, is accompanied by a corresponding increase in macroturbulence.

The higher turbulent broadening indicates that  $\epsilon$  Tau is slightly more evolved than  $\gamma$  Tau. The difference in line-width is a more subtle example of the much more dramatic spectral differences observed between the giant stars,  $\mu$  Peg and  $\lambda$  Peg (Smith 1998). Knowing the parallaxes of our two stars, now accurately determined by the Hipparcos satellite (ESA 1997), and the integrated flux above the Earth's atmosphere, determined

by means of the infrared flux method (Blackwell & Lynas-Gray 1998), we obtain the luminosities given below:

|                              | $\gamma$ Tau          | $\epsilon$ Tau        |
|------------------------------|-----------------------|-----------------------|
| Parallax (mas)               | $21.17 \pm 1.17$      | $21.04 \pm 0.82$      |
| Flux ( $\text{W m}^{-2}$ )   | $1.14 \times 10^{-9}$ | $1.28 \times 10^{-9}$ |
| Luminosity ( $L/L_{\odot}$ ) | 79.7                  | 90.5                  |

These luminosities are typical of stars on their first ascent of the Red Giant Branch.

If both stars have a mass of  $2.3 M_{\odot}$ , the usual relation between  $M$ ,  $L$ ,  $g$  and  $T_{\text{eff}}$  yields  $\log g = 2.63$  for  $\gamma$  Tau and  $\log g = 2.57$  for  $\epsilon$  Tau. These values are very close to the values,  $2.65 \pm 0.2$  and  $2.45 \pm 0.2$  respectively, determined from the profile of the Ca II 8542 Å line (Smith & Ruck 1997). In reality, we might expect the mass of  $\epsilon$  Tau to be slightly higher given its slightly more evolved state and the likelihood that the two stars were formed contemporaneously. On the other hand, if the slightly deeper 8542 Å line profile in  $\epsilon$  Tau is really the consequence of a surface gravity lower in  $\log g$  by 0.2 dex, as suggested by Smith & Ruck (1997), the two stars cannot have been formed at the same time:  $\epsilon$  Tau must be slightly less massive and a little older. Baliunas et al. (1983), in a study of chromospheric and coronal emissions from Hyades giants, found greater chromospheric emission strengths in  $\gamma$  Tau than in  $\epsilon$  Tau using the Mg II h,k and Ca II K line cores as indicators. This activity can also produce in-filling of the Ca II infrared triplet line cores but high-resolution studies of the 8542 Å line profile in the active dwarf stars  $\xi$  Boo A and  $\epsilon$  Eri (Ruck & Smith 1995; Drake & Smith 1993) indicate that the in-filling only occurs within  $\pm 2$  Å of the line centre. This is unlikely to provide an explanation for the slightly shallower 8542 Å line absorption observed in  $\gamma$  Tau which extends over a much greater part of the profile. However, a slightly different temperature structure throughout the photosphere, arising from some cause other than a difference in surface gravity, could produce the effect. It would be useful to have further observations so as to check to what extent the chromospheric activity is a transient phenomenon. The mild activity so far observed in  $\gamma$  Tau would be unlikely to cause magnetic effects in other spectral lines.

## 6. Conclusion

A detailed study of two spectral regions in the giant stars  $\gamma$  Tau and  $\epsilon$  Tau, which have very similar effective temperatures, has revealed that turbulent broadening of line profiles in  $\epsilon$  Tau is slightly greater than that in  $\gamma$  Tau. Temperature dependent features indicate that the effective temperature of  $\epsilon$  Tau is less than that of  $\gamma$  Tau by  $80 \pm 20$  K in agreement with recent determinations by the infrared flux method. Although the micro/macroturbulence model, adopted here, is a very crude approximation to the real turbulent velocity fields in stars, it suc-

ceeds in reproducing the observed effects. An analysis of iron and calcium lines yields logarithmic abundances, relative to the Sun, which are consistent with recent more extensive analyses. The derived microturbulence values of around  $1.4 \text{ km s}^{-1}$  are similar to those found, using spectra of comparable quality, for other stars at an evolutionary stage near the lower end of the Red Giant Branch.

*Acknowledgements.* I wish to thank the Director of the McDonald Observatory for granting facilities for our observations. It is a particular pleasure to record my gratitude to Professor D.L. Lambert and Dr. J. Tomkin of the University of Texas for considerable help with observations and data reduction, and for warm hospitality during my visit. Dr. M.J. Ruck gave substantial help with the initial stages of data reduction. I gratefully acknowledge the generosity of Professor B. Gustafsson in making the MARCS suite of programs available to UK astronomers. Data analysis and document preparation at Oxford were undertaken using packages available on the STARLINK network which is supported by the Particle Physics and Astronomy Research Council (PPARC) of the U.K. I acknowledge support from the Panel for Allocation of Telescope Time of the former Science and Engineering Research Council while carrying out this work.

## References

- Baliunas S.L., Hartmann L., Dupree A.K., 1983, ApJ 271, 672  
 Bell R.A., Eriksson K., Gustafsson B., Nordlund Å, 1976, A&AS 23, 37  
 Blackwell D.E., Lynas-Gray A.E., 1998, A&AS 129, 505  
 Blackwell D.E., Petford A.D., Shallis M.J., Simmons G.J., 1982, MNRAS 199, 43  
 Drake J.J., Smith G., 1991, MNRAS 250, 89  
 Drake J.J., Smith G., 1993, ApJ 412, 797  
 ESA, 1997, The Hipparcos Catalogue, ESA SP-1200  
 Gratton R.G., Ortolani S., 1986, A&A 169, 201  
 Gray D.F., 1975, ApJ 202, 148  
 Gray D.F., 1982a, ApJ 258, 201  
 Gray D.F., 1982b, ApJ 262, 682  
 Gray D.F., 1989, ApJ 347, 1021  
 Gray D.F., 1992, The Observation and Analysis of Stellar Photospheres. 2nd ed., Cambridge Univ. Press  
 Gray D.F., Endal B., 1982, ApJ 254, 162  
 Griffin R., 1969, MNRAS 143, 381  
 Helfer H.L., Wallerstein G., 1964, ApJS 9, 81  
 Holweger H., Müller E.A., 1974, Solar Phys. 39, 19  
 Jørgensen U.G., Larsson M., 1990, A&A 238, 424  
 Kurucz R.L., Furenlid I., Brault J.W., Testerman L., 1984, Solar Flux Atlas from 296 to 1300 nm. National Solar Observatory Solar Atlas no. 1  
 Perryman A.C., Brown A.G.A., Lebreton Y., Gómez A., Turon C., et al., 1998, A&A 331, 81  
 Raassen A.J.J., Uylings P.H.M., 1998, A&A 340, 300  
 Ruck M.J., Smith G., 1995, A&A 304, 449  
 Smith G., 1998, A&A 339, 531  
 Smith G., Lambert D.L., Ruck M.J., 1992, A&A 263, 249  
 Smith G., Raggett D.St.J., 1981, J. Phys. B 14, 4015  
 Smith G., Ruck M.J., 1997, A&A 324, 1091